

Supplementary Materials for

Denervation suppresses gastric tumorigenesis

Chun-Mei Zhao, Yoku Hayakawa, Yosuke Kodama, Sureshkumar Muthupalani, Christoph B. Westphalen, Gøran T. Andersen, Arnar Flatberg, Helene Johannessen, Richard A. Friedman, Bernhard W. Renz, Arne K. Sandvik, Vidar Beisvag, Hiroyuki Tomita, Akira Hara, Michael Quante, Zhishan Li, Michael D. Gershon, Kazuhiro Kaneko, James G. Fox, Timothy C. Wang,* Duan Chen*

*Corresponding author. E-mail: duan.chen@ntnu.no (D.C.); tcw21@columbia.edu (T.C.W.)

Published 20 August 2014, *Sci. Transl. Med.* **6**, 250ra115 (2014)

DOI: 10.1126/scitranslmed.3009569

The PDF file includes:

Materials and Methods

Fig. S1. Flowchart showing the animal study design.

Fig. S2. Anterior UVT in mice.

Fig. S3. Body weight of male and female INS-GAS mice after surgery.

Fig. S4. Thickness of the gastric oxyntic mucosa after surgery in INS-GAS mice.

Fig. S5. Pathological scores for the stomach after surgery in INS-GAS mice.

Fig. S6. Pathological scores for the stomach after Botox injection in INS-GAS mice.

Fig. S7. Wnt signaling in INS-GAS mice compared with wild-type mice.

Fig. S8. Altered signaling pathways after vagotomy in INS-GAS mice.

Fig. S9. Wnt and Notch signaling pathways after vagotomy in INS-GAS mice.

Fig. S10. Immunostaining of CD44 after vagotomy in INS-GAS mice.

Fig. S11. Numbers of CD44-immunoreactive cells after Botox treatment \pm vagotomy in INS-GAS mice.

Fig. S12. Tumor regeneration in the stomach after vagotomy in INS-GAS mice.

Fig. S13. Wnt signaling KEGG pathway in M₃KO mice compared with wild-type mice.

Fig. S14. Altered signaling pathways in human gastric cancer tissue compared with adjacent noncancerous tissue.

Fig. S15. Gastric stump cancer after distal gastrectomy with or without vagotomy.

Fig. S16. Effect of 5-FU and oxaliplatin in INS-GAS mice.

Table S1. Animal experimental groups.

Table S2. Cohorts of gastric cancer patients.

Table S3. List of qRT-PCR primers used in this study.

Supplementary Materials and Methods

Animals

The insulin-gastrin (INS-GAS) transgenic mice were generated by Dr. T.C. Wang (18), and imported to Norway by Dr. D. Chen for these studies. Animals were further bred through sibling mating for more than 20 generations. 829 INS-GAS mice have been examined during the past 9 years. The percentage of the mice without preneoplastic lesions was 3.7% at 6 months of age, and the prevalence of spontaneous gastric cancer increased from 75% (at the beginning of this study in Jan. 2005) to 100% (May 2013) at 12 months of age without an additional infection with *Helicobacter pylori*. 187 INS-GAS mice were examined at 1 to 20 months of age during 2005, and 61 mice were found to have gastric tumors after 9 months of age (see Fig. 1A: the tumor prevalence at the lesser or greater curvature of the stomach). During 2012, 139 INS-GAS mice were examined at 12 months of age and all mice had gastric tumors. M₃KO mice were obtained from Dr. Koji Takeuchi at Kyoto Pharmaceutical University (45). M₃KO mice had higher water intake than age- and sex-matched wild type mice (14.62±1.71 vs. 6.48±1.00 mL/100 g body weight/24 hours, Means ± SEM (N=8), $p = 0.01$ (Student's t test). The chemically-induced gastric cancer model was established according to our previous report (22). In brief, mice were exposed to N-Methyl-N-nitrosourea (MNU, Sigma Chemicals), which was dissolved in distilled water at a concentration of 240 ppm and freshly prepared twice per week for administration in drinking water in

light-shielded bottles *ad libitum*. Starting at 4 weeks of age, mice were given drinking water containing MNU on alternate weeks for a total of 10 weeks. *H. pylori* infection was induced in H⁺/K⁺-ATPase-IL-1 β mice (23) by inoculation with pre-mouse Sydney strain 1 [PMSS1]. Three inocula (0.2 mL of *Hp*, 10¹⁰ colony-forming units/mL) were delivered every other day by oral gavage using a sterile gavage needle.

In the present study, animals were housed 3-4 mice per cage on wood chip bedding with a 12-hour light/dark cycle, room temperature of 22°C and 40-60% relative humidity. INS-GAS mice and FVB wild-type (WT) mice were housed at the standard housing conditions in a specific pathogen-free environment. M₃KO mice, *Hp*-infected H⁺/K⁺-ATPase-IL-1 β mice, and WT controls (C57BL/6 mice, Taconic, Denmark) were housed in a guaranteed animal facility at Comparative Medicine Core Facility at Norwegian University of Science and Technology. All the mice had free access to tap water and standard pellet food (RM1 801002, Scanbur BK AS). Animal experiments were approved by the Norwegian National Animal Research Authority (Forsøksdyrutvalget, FDU) and by the Columbia University Institutional Animal Care and Use Committee (IACUC).

Experimental designs

581 mice were divided into 14 experimental groups (Table S1). In each experiment, mice were randomly divided into different subgroups. The animals, samples, and treatments were coded until the data were analyzed.

In the 1st experiment, 107 INS-GAS mice underwent bilateral truncal vagotomy with pyloroplasty (VTPP) (6 males, 19 females), pyloroplasty alone (PP) (7 males, 18 females), unilateral anterior truncal vagotomy (UVT) (11 males, 19 females), or sham operation (11 males, 16 females) at 6 months of age. Six months after surgery (at 12 months of age), the animals were euthanized, and the anterior and posterior parts of the stomachs were collected for histopathological and immunohistochemical analyses.

In the 2nd experiment, 20 WT mice (FVB, the same genetic background as INS-GAS mice) were exposed to MNU for one week every other week for 5 cycles (10 weeks). At 3.5 months of age, half of the MNU-treated mice underwent VTPP and the other half underwent a sham operation (PP). All the mice were euthanized at 13 months of age, and the stomachs were examined macroscopically and collected for histopathological analysis.

In the 3rd experiment, 24 H⁺/K⁺-ATPase-IL-1 β mice (14 males and 10 females, backcrossed to C57BL/6 for 10 generation) were inoculated with *Hp* at 3.5 months of age. At 12 months of age, half of the infected mice underwent UVT and the other half underwent a sham operation (laparotomy). All the mice were euthanized 6 months later. The stomachs were examined macroscopically and collected for histopathological analysis.

In the 4th experiment, 16 INS-GAS mice (5 males and 11 females) at 6 months of age underwent unilateral Botox treatment and were euthanized at 12 months of age. The anterior and posterior parts of the stomachs were collected for histopathological analysis.

In the 5th experiment, 64 INS-GAS mice at 8 months (7 males and 10 females), 10 months (6 males and 8 females) and 12 months (6 males and 6 females) of age underwent UVT, and 21 age-matched mice (8 males and 13 females) had no surgery. At 18 months of age, all surviving mice including 12 (6 males and 6 females) from the 8-month group, 9 from the 10-month group (3 males and 6 females), 8 from the 12-month group (4 males and 4 females), and 10 from the un-operated group (4 males and 6 females) were euthanized, and the anterior and posterior parts of the stomachs were collected for histopathological analysis and genome-wide gene expression profiling analysis. Survival analysis was also performed.

In the 6th experiment, 26 INS-GAS mice at 12 months of age underwent Botox treatments (only anterior or both anterior and posterior sides of the stomach with or without UVT) or vehicle injection (both anterior and posterior sides of the stomach). Mice were euthanized at 14 months of age. Both the anterior and posterior parts of the stomachs were collected for histopathological analysis.

In the 7th experiment, 133 INS-GAS mice at 12-14 months of age received no treatment (6 males and 6 females), saline (5 males and 5 females), 5-fluorouracil (5-FU) (5 males and 5 females), oxaliplatin (5 males and 8 females), saline + unilateral Botox treatment (4 males

and 6 females), unilateral Botox treatment + 5-FU (4 males and 6 females), unilateral Botox treatment + oxaliplatin (6 males and 7 females), sham operation (laparotomy) + 5-FU + oxaliplatin (6 males and 9 females), unilateral Botox treatment + 5-FU + oxaliplatin (11 males and 13 females), or UVT+ 5-FU + oxaliplatin (6 males and 10 females). Denervation treatment was applied to only half of the stomach, such that the non-denervated half of the stomach in each animal served as a control, either as chemotherapy only or as an untreated control. All mice were euthanized 2 months after starting the treatments, except for mice that died before the end of study, and both the anterior and posterior parts of the stomachs were collected for histopathological analysis. Survival analysis was also performed.

In the 8th experiment, 16 INS-GAS mice at 6 months of age underwent UVT and were euthanized at 2 months (1 male and 4 females), 4 months (2 males and 3 females), or 6 months (2 males and 4 females) postoperatively. The anterior and posterior parts of the stomachs were collected for genome-wide gene expression profiling.

In the 9th experiment, 44 INS-GAS mice at 12-14 months of age received saline (3 males and 3 females), 5-FU + oxaliplatin (5 males and 8 females), darifenacin (6 males and 6 females), or a combination of 5-FU + oxaliplatin and darifenacin (8 males and 5 females). Two months after starting the treatments, the mice were euthanized, and both the anterior and posterior parts of the stomachs were collected for histopathological analysis.

In the 10th experiment, both INS-GAS mice (6 males and 6 females) and WT mice (10 males and 10 females) were subjected either to UVT or no treatment. Six months after surgery (at 12 months of age), the animals were euthanized and the anterior and posterior parts of the stomachs were collected for gene expression analysis.

In the 11th experiment, 12 MNU-treated mice (6 males and 6 females) were subjected to PP or VTPP at 6 months of age and euthanized 4 months later. The stomachs were collected for qRT-PCR analysis.

In the 12th experiment, 7 M₃KO mice (4 males and 3 females) and 13 WT mice (5 males and 8 females) (C57BL/6, the same genetic background as M₃ KO mice) were exposed to MNU and euthanized at 11 months of age. The stomachs were examined macroscopically and were collected for histopathological analysis.

In the 13th experiment, 37 mice (20 males, 17 females) at 12-18 months of age underwent a topical application of acetic acid on the anterior side of the stomach with or without simultaneous UVT and were euthanized 1 week (5 males, 7 females), 2 weeks (3 males, 9 females), or 3 weeks (12 males, 1 female) later, and the anterior parts of the stomachs were collected for histopathological analysis.

In the 14th experiment, 10 Lgr5-GFP mice (all males) were treated with MNU at 2 months of age, subjected to PP or VTPP at 19 weeks of age, and euthanized at 25 weeks of age.

Animal surgery

All surgical procedures were performed under isoflurane inhalation anesthesia (2-3 %), with buprenorphine (0.1 mg/kg subcutaneously) given as postoperative analgesia. The abdominal cavity was accessed through a midline incision. The sham operation consisted of a laparotomy with mild manipulation of organs, including identification of the vagus nerve. PP was done by longitudinal incision of the pyloric sphincter followed by transverse suturing. VTPP was performed by subdiaphragmatic dissection of both the anterior and posterior vagal trunks and simultaneous PP to prevent post-vagotomy delayed gastric emptying. In UVT, only the anterior truncal vagus nerve was cut (Fig. S2), leading to a specific vagal denervation of the anterior aspects of the stomach, with preserved pyloric function making PP unnecessary. Sample collection was done under inhalation anesthesia as described, and the animals were euthanized by exsanguination while still under anesthesia.

Botox treatment

Botox 100 U (Botox Allergan Inc.) was dissolved in 0.9% cold saline and 1% methylene blue (to visualize the injection), achieving a concentration of 0.25 U of Botox/mL. The Botox solution was injected subserosally along the greater curvature into the anterior (unilateral Botox treatment) or both anterior and posterior sides (bilateral Botox treatment) of the stomach (only the corpus area where tumor developed) at the dose of 0.05 U/mouse (0.2

mL/mouse) or 0.1 U/mouse (0.4 mL/mouse), respectively, once per month until the end of the study. In the control group, the vehicle solution was prepared with 0.9% saline and 1% methylene blue and injected into both anterior and posterior sides of the stomach (only the corpus area where tumor developed) at a volume of 0.4 mL/mouse.

Chemotherapy and M₃ receptor antagonist treatment

5-Fluorouracil (5-FU, Flurablastin, Pfizer, Inc.) was diluted in saline and given at a dose of 25 mg/kg in a volume of 1 mL. Oxaliplatin (Hospira, Inc.) was diluted in saline and given at 5 mg/kg in 1 mL. Combination of 5-FU (25 mg/kg in 0.5 mL) and oxaliplatin (5 mg/kg in 0.5 mL) was given at the same time, but the drugs were injected separately. Chemotherapy was given by intraperitoneal injection weekly in 2 cycles, namely 3 injections in the 1st month (starting one week after the 1st Botox, UVT, or the 1st osmotic mini-pump implantation), and 3 injections in the 2nd month (starting at one week after the 2nd Botox, no UVT, or the 2nd mini-pump). Age- and sex-matched mice received intraperitoneal injection of saline (1 mL) as controls. The injection needle was 27 G. The dosages and regimens were made based on our pilot experiments for selecting the doses. There was no effect on tumor size by 5-FU or oxaliplatin alone (Fig. S16).

Darifenacin hydrobromide (Santa Cruz Biotechnology) was given at a dose of 1 mg/kg/h for 2 months via an osmotic mini-pump (ALZET 2006) as reported previously (48).

Tumor regeneration model

Topical application of acetic acid was found to promptly cause necrosis in the tumor tissue in INS-GAS mice. Under isoflurane anesthesia, the stomach was exposed through a midline abdominal incision, and 60% acetic acid was topically applied to the serosa of the anterior side of the stomach for 60 seconds using a 5 mm internal diameter cylindrical metal mold. In the experiment combining acetic acid-induced necrotic ulcers with UVT, the mice underwent acetic acid application during the UVT surgery.

Pathological and immunohistochemical analyses

The stomachs were removed, opened along the greater curvature, washed in 0.9% NaCl, and pinned flat on a petri-dish-silicone board. Each stomach was photographed digitally; the tumor profiles in both anterior and posterior sides of the stomach were drawn separately and subjected to morphometric analysis of the volume density (expressed as the percentage of glandular volume occupied by the tumor) using point-counting technique with a test grid comprised of a 1.0 cm square lattice. This grid was placed over each photograph (40 x 30 cm²), and the numbers of test points overlying the tumor and gastric glandular area were determined. The samples for histology comprised multiple linear strips along the greater curvature of the stomach wall, extending from the squamocolumnar junction through the

antrum. Samples were fixed in 4% formaldehyde for 8-12 hours at room temperature and embedded in paraffin. Sections (4 μm thick) were stained with hematoxylin and eosin. Pathological evaluation was performed by comparative pathologists and a histologist who were blinded to the sample source. The gastric lesions were scored on an ascending scale from 0 to 4, using criteria adopted from previous reports (21). Inflammation scoring were assigned for patchy infiltration of mixed leukocytes in mucosa and/or submucosa (1), multifocal-to-coalescing leukocyte infiltration not extended below submucosa (2), marked increase in leukocytes with lymphoid follicles +/- extension into tunica muscularis (3), or effacing transmural inflammation (4). The epithelial defects were defined as gland dilatation, surface erosions and gland atrophy, and ulceration and fibrosis. Immunohistochemistry was performed using a DAKO AutoStainer (Universal Staining System with DAKO EnVision System, Dako). Antibodies used were Ki67 (1:100; code M7249, Dako), PCNA (1:100, code M0879, Dako), CD44 (1:100, code 550538, BD Pharmingen), CD44V6 (1:200, code AB2080, Millipore), PGP9.5 (1:1000, code Z5116, Dako, and code 7863-0504, AbD Serotec), peripherin (1:500, code AB1530, Millipore), β -catenin (1:500, code 610654, BD Transduction Laboratories), Alexa Fluor 488 Phalloidin (1:200, code A12379, Life Technologies), Alexa Fluor 555 Goat Anti-Rabbit IgG (H+L)(1:200, code A21428, Life Technologies). Cellular proliferation is expressed as the number of Ki67 or PCNA immunoreactive cells/gland. There was no difference between the two markers between two

labs (TW and DC). Slides were visualized on a Nikon TE2000-U and representative microhistophotos were taken. Positive-stained cells with nuclei were counted only in dysplastic glands, with least 50 glands counted per animal in a blinded fashion, and results are expressed as numerical densities (number of cells per gland, number of cells per 10 glands or per object field). Positive-stained nerves were quantitated by ImageJ software and are expressed as positive area per total mucosal area.

Vagus nerve fibers and terminals in the mouse stomach traced with carbocyanine dye (DiI)

The esophagus, diaphragm and stomach were removed from adult mice and fixed for 3 days with formaldehyde. DiI crystals were placed on the anterior and posterior thoracic vagal trunks about 1 cm above the diaphragm, which was left undisturbed. The preparation was incubated at 37°C in PBS containing 0.5% sodium azide in a sealed container for 3 months. After incubation, the stomach was opened along the greater curvature, the mucosa and submucosa were removed, and the preparations were mounted, serosal side up, in buffered glycerol for microscopic examination. DiI fluorescence was viewed with a Leica CTR6000 microscope equipped with a cooled CCD camera and computer assisted video imaging. The entire gastric wall was scanned with a 2.5x objective, and a montage was made from the resulting images. In order to observe the density of DiI-labeled vagal fibers within the

myenteric plexus, additional images were obtained at higher magnification in the lesser curvature close to the esophagogastric junction and in the greater curvature. The density of DiI-labeled fibers was estimated by point counting technique. A test system comprising a 1.0 cm square lattice was placed over each photograph, and the numbers of test points overlying the DiI-labeled fibers and the visual field were determined.

RNA isolation, gene expression profiling by microarray, qRT-PCR arrays and qRT-PCR in mice and humans

The collected mouse and human stomach samples were kept frozen at -80°C until further processing. Total RNA from the frozen stomach samples was isolated and purified using an Ultra-Turrax rotating-knife homogenizer and the mirVana miRNA Isolation Kit (AM1560, Ambion) according to the manufacturer's instructions. Concentration and purity of total RNA were assessed using a NanoDrop photometer (NanoDrop Technologies, Inc.). The A260/280 ratios were 2.05 ± 0.01 for mouse samples and 1.96 ± 0.10 for human samples (mean \pm SEM). RNA integrity was assessed using a Bioanalyzer (Agilent Technologies) and found satisfactory, with RNA integrity number (RIN) values 9.1 ± 0.1 for mouse samples, and 8.7 ± 0.9 for human samples (means \pm SEM). The microarray gene expression analysis followed standard protocols, analyzing 300 ng total RNA per sample with the Illumina MouseWG-6 and HumanHT-12 Expression BeadChips (Illumina). Microarray data were confirmed by

qRT-PCR array (RT² Profiler PCR Array, SABiosciences) (StepOnePlus™, Applied Biosystems). Mouse microarray data were deposited in the Gene Expression Omnibus (GEO accession no. GSE30295), and human data in ArrayExpress (accession no. E-MTAB-1338). Longitudinal strips of gastric tissue from the anterior wall as well as the posterior wall were harvested and snap-frozen in dry ice and kept in a -80°C freezer until processed for analysis. Total RNA was extracted with Nucleospin RNA II kit (Clontech), and cDNA was synthesized by Superscript III First-strand Synthesis System for RT-PCR (Invitrogen). See Table S3 for primer sequences used. Expression levels of indicated genes were quantified by real-time PCR assays with SYBR Green dye and the Applied Biosystems 7300 Real Time PCR System.

Fluorescence-activated cell sorting (FACS)

Single epithelial cells were isolated from *Lgr5*-GFP mouse stomachs. Isolated crypts were dissociated with TrypLE Express (Invitrogen) including 1 mg/ml DNase I (Roche Applied Science) for 10 minutes at 37°C. Dissociated cells were passed through a 20-µm cell strainer, washed with 2% FBS/PBS, and sorted by FACS (BD FACSAria Cell Sorter III). Viable single epithelial cells were gated by forward scatter, side scatter and a pulse-width parameter, and negative staining for propidium iodide. Cells expressing high and low levels of GFP and

GFP-negative cells were sorted separately, and RNA was isolated by using RNAqueous-Micro Kit (Ambion).

***In vitro* culture system**

Wild-type (WT), Ubiquitin C-green fluorescent protein (UBC-GFP), or Gt(ROSA)26Sortm4(ACTB-tdTomato,-EGFP)Luo/J mice (The Jackson laboratory) were used for *in vitro* culture. Gastric gland isolation and culture were performed as described previously (9), with minor modifications. Stomachs removed from WT and M₃KO mice were opened longitudinally, chopped into approximately 5 mm pieces, and incubated in 8 mM EDTA in PBS for 60 minutes on ice. The tissue fragments were vigorously suspended, yielding supernatants enriched in gastric glands. Gland fractions were centrifuged at 900 rpm for 5 minutes at 4°C and diluted with advanced DMEM/F12 (Invitrogen) containing B27, N2, 1 μM n-Acetylcysteine, 10 mM HEPES, penicillin/streptomycin, and Glutamax (all Invitrogen). Glands were embedded in extracellular matrix (Fisher Bioservices/NCI Frederick Central Repository) and 400 crypts/well were seeded on pre-warmed plates. Advanced DMEM/F12 medium containing 50 ng/mL EGF, 100 ng/mL Noggin, and 1 μg/mL R-spondin1 was applied. Wnt3a (PeproTech) was added at 100 ng/mL when indicated. Growth factors were added every other day, and the entire medium was changed twice a week. Passage was performed at day 7 as described previously (9). Mouse primary neuronal cells were prepared following the protocol described previously (33). Neuronal cells were

mixed with extracted gastric crypts in the extracellular matrix at the ratio of crypt:neuron 1:5. The enteric nervous system was isolated from guinea pigs as described previously (34). Botox, scopolamine hydrochloride, and pilocarpine hydrochloride (Sigma) were dissolved in PBS and added in the cultured medium every other day. The images of gastric organoids were acquired using fluorescent microscopy (Nikon, TE2000-U) and two-photon microscopy (Nikon, A1RMP). Isolation of mRNA from cultured organoids was performed with a NucleoSpin RNA XS kit (Clontech Laboratories Inc.) according to manufacturer's instructions. The first-strand complementary DNA was synthesized using the ImProm-II Reverse Transcription System (Promega). Amplification was performed using the ABI PRISM 7300 Quantitative PCR System (Applied Biosystems).

Patients and methods

Three cohort studies were included (Table S2). In the 1st study, human stomach specimens (both tumors and the adjacent non-tumor tissues) were taken immediately after gastrectomy from 17 patients during 2005 to 2010 at St. Olav's University Hospital, Trondheim, Norway for gene expression profiling analysis. All patients were diagnosed histologically as primary gastric carcinoma of stage I-IV. 10 of 17 patients were *H. pylori* positive at the time of surgery. In the 2nd study, human stomach tissues were obtained from 120 gastric cancer patients who underwent curative surgical resection from 2001 to 2008 at Gifu University

Hospital, Gifu, Japan. All patients were diagnosed histologically as primary gastric carcinoma of stage II, III, or IV. Immunohistochemical analysis of the nerve density was performed with PGP9.5 antibody. Low and high expression of PGP9.5 were defined with respect to the median of the volume density of PGP9.5. In the 3rd study, clinical data of 37 patients with gastric stump cancer (GSC) who had received distal gastrectomy with or without vagotomy during 1962 to 1995 at the National Cancer Center Hospital East, Chiba, Japan were evaluated. GSC was defined as gastric cancer that occurred ≥ 5 years (from 5 to 36 years) after curative distal gastrectomy, regardless of the original benign or malignant disease. GSC included in this study was adenocarcinoma infiltrating the mucosal or submucosal layer. The tumor location was recorded according to the recommendation by the Japanese Gastric Cancer Association: anterior or posterior wall, or lesser or greater curvature (Fig. S15). All the study protocols were approved by the ethics committees in Japan and Norway, and written informed consent was obtained from patients.

Data analysis and statistics

Values were expressed as means \pm SEM. Pairwise comparisons between experimental groups and between anterior and posterior sides of the stomach were performed with the paired and unpaired *t*-test as appropriate. All tests were two sided with a significance cutoff of 0.05. Comparisons between more than 2 groups were performed by ANOVA, followed by

Dunnett's test or Tukey's test as appropriate. Comparisons with categorical independent variables were performed using Fisher's exact test. Kaplan-Meier survival curves were calculated and were analyzed by the Cox proportional hazard method. Tumor prevalence/incidence was analyzed by Fisher's exact test. Affymetrix microarray data were normalized using RMA, and Illumina microarray data was analyzed using Lumi. Both qRT-PCR and microarray data were analyzed on the \log_2 scale. The significance of differential expression of qRT-PCR data was analyzed using parametric frequentist statistics, and microarray data were analyzed using the empirical Bayesian method implemented in Limma. Gene expression profiles from both microarray and qRT-PCR were analyzed independently by a paired robust *t*-test for mouse samples or a paired *t*-test for human samples. Paired *t*-statistics were computed by fitting a linear robust or non-robust regression to the anterior and posterior stomach samples within each mouse or to the cancer and the adjacent non-cancerous tissue samples within each patient. For microarray data, transcripts with Benjamini-Hochberg false discovery rates less than 0.05 were considered to be differentially expressed. Regulated KEGG (Kyoto Encyclopedia of Genes and Genomes) pathways were identified using Signaling Pathway Impact Analysis. All of the above calculations were performed in the R/Bioconductor software environment.

Supplementary figures and tables

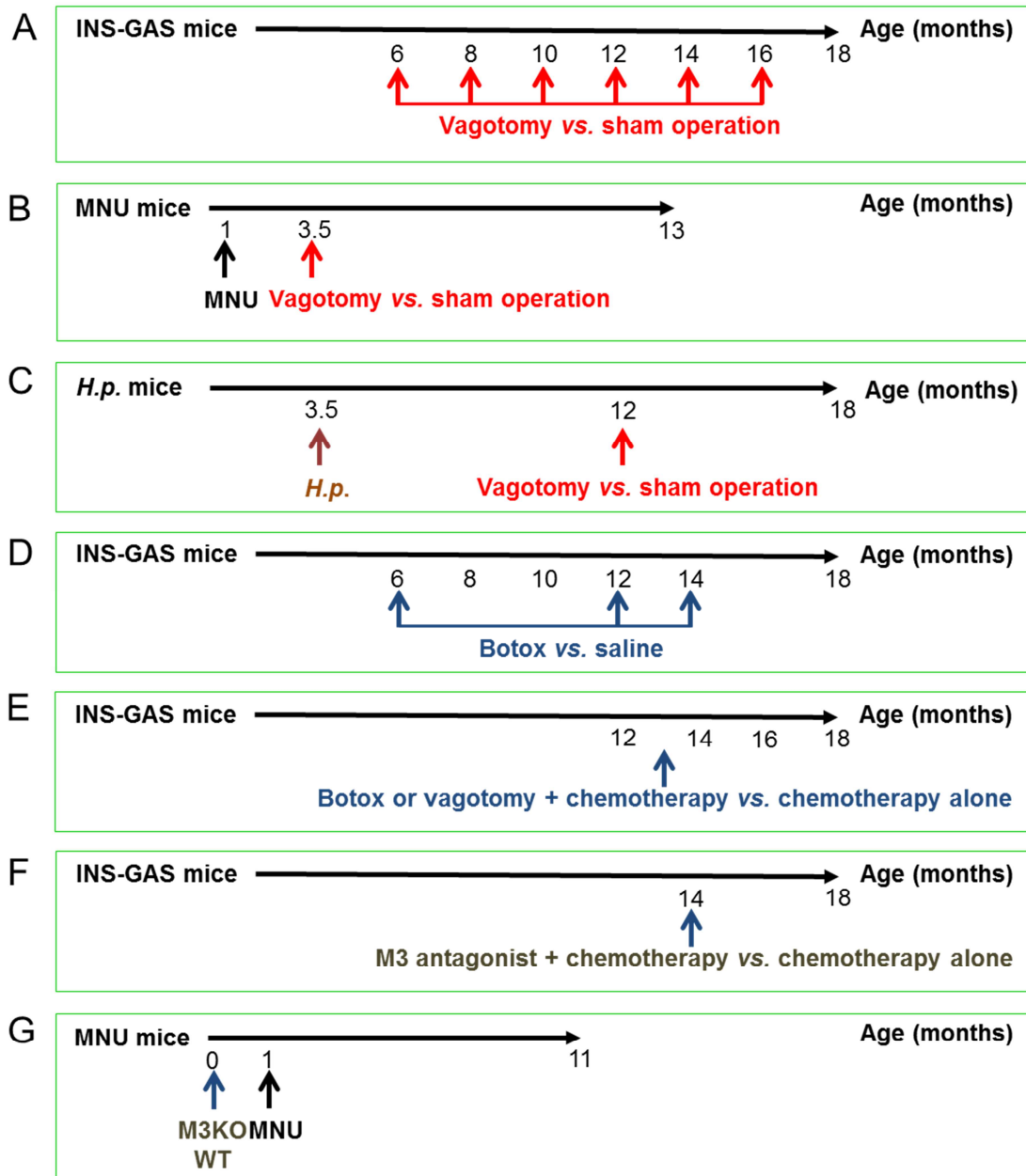


Fig. S1. Flowchart showing the animal study design.

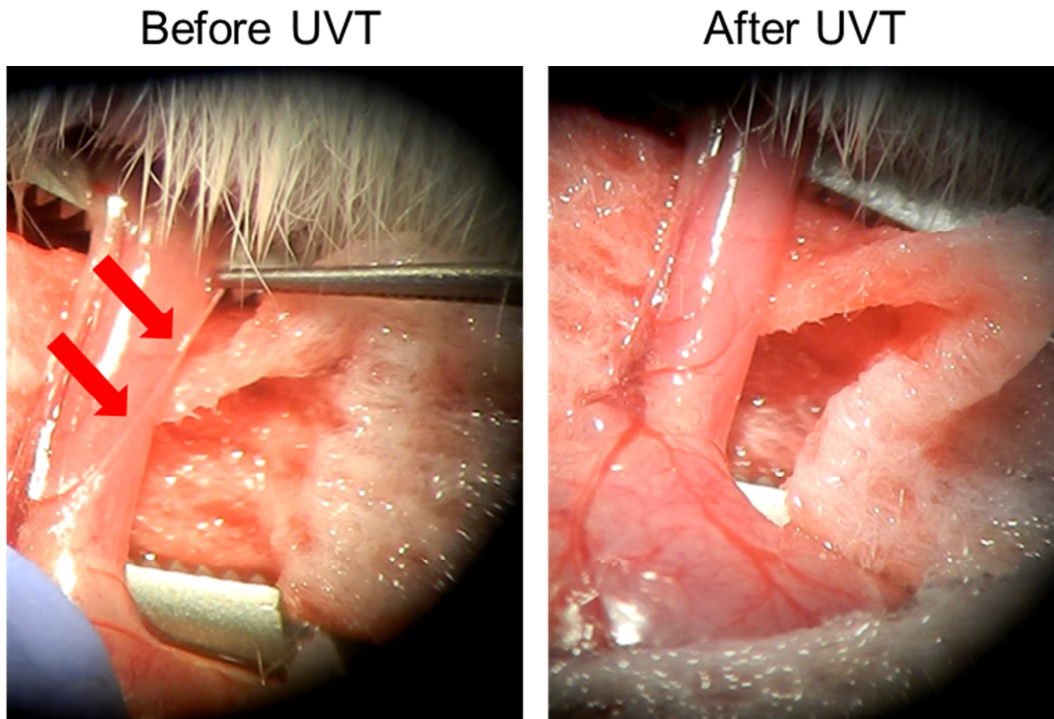


Figure S2: Anterior UVT in mice. Photographs showing dissected vagus nerve (indicated by arrows) before and after anterior unilateral truncal vagotomy (UVT) are shown.

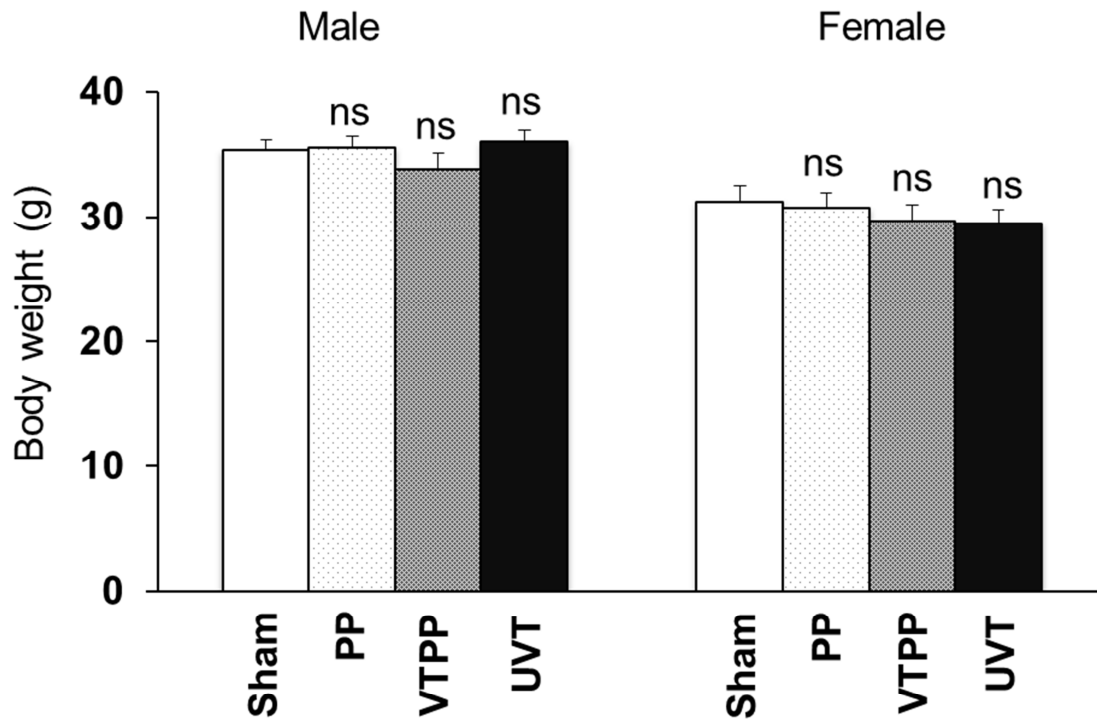


Figure S3: Body weight of male and female INS-GAS mice after surgery. Body weight of sham (Sham), pyloroplasty (PP), bilateral vagotomy with pyloroplasty (VTPP), and anterior unilateral vagotomy (UVT)-operated INS-GAS mice at 12 months of age (6 months postoperatively). Means \pm SEM. ns: not significantly different between Sham ($N = 11$ males, 16 females) and PP ($N = 7$ males, 18 females), VTPP ($N = 6$ males, 19 females), or UVT ($N = 11$ males, 19 females) (Dunnett's test).

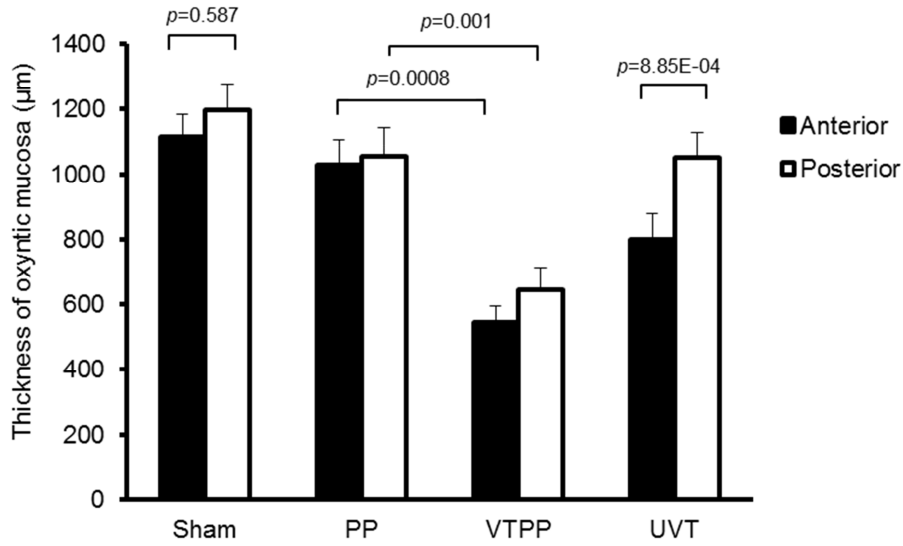


Figure S4: Thickness of the gastric oxyntic mucosa after surgery in INS-GAS mice.

Thickness of the oxyntic mucosa in sham (Sham), pyloroplasty (PP), bilateral vagotomy with pyloroplasty (VTPP), and anterior unilateral vagotomy (UVT)-operated INS-GAS mice at 12 months of age (6 months postoperatively). Means \pm SEM. Tukey test: between PP ($N = 25$) and VTPP ($N = 25$). Paired t test: between anterior vs. posterior sides within Sham ($N = 27$) and UVT ($N = 30$).

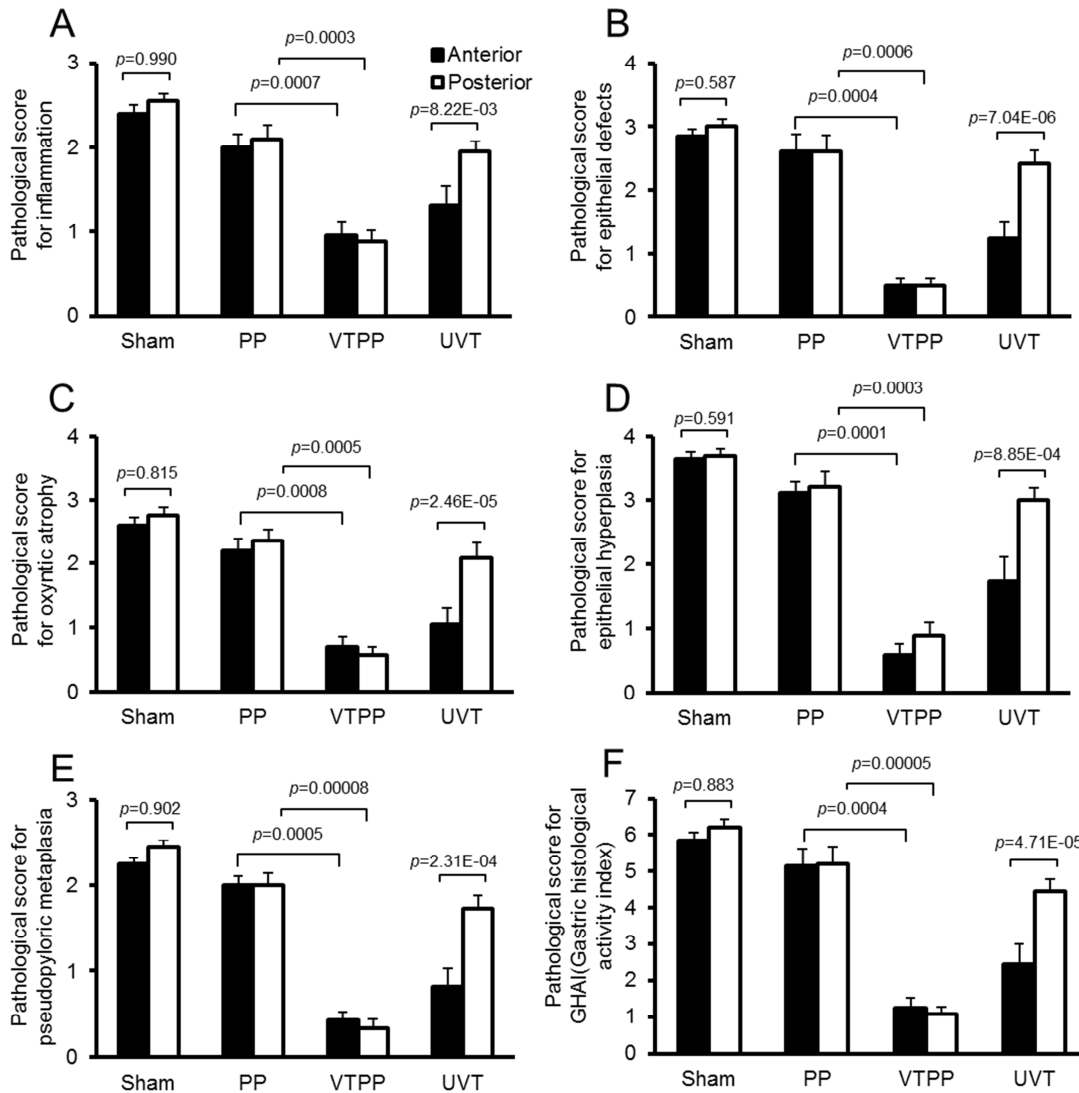


Figure S5: Pathological scores for the stomach after surgery in INS-GAS mice. Pathological scores for inflammation (A), epithelial defects (B), oxyntic atrophy (C), epithelial hyperplasia (D), pseudopyloric metaplasia (E), and GHAI (gastric histological activity index) (F) in sham (Sham), pyloroplasty (PP), bilateral vagotomy with pyloroplasty (VTPP), and anterior unilateral vagotomy (UVT)-operated INS-GAS mice at 12 months of age (at 6 months after surgery). Means \pm SEM. Tukey test: between PP ($N = 25$) and VTPP ($N = 25$). Paired t test:

between anterior vs. posterior sides within Sham ($N = 27$) and UVT ($N = 30$).

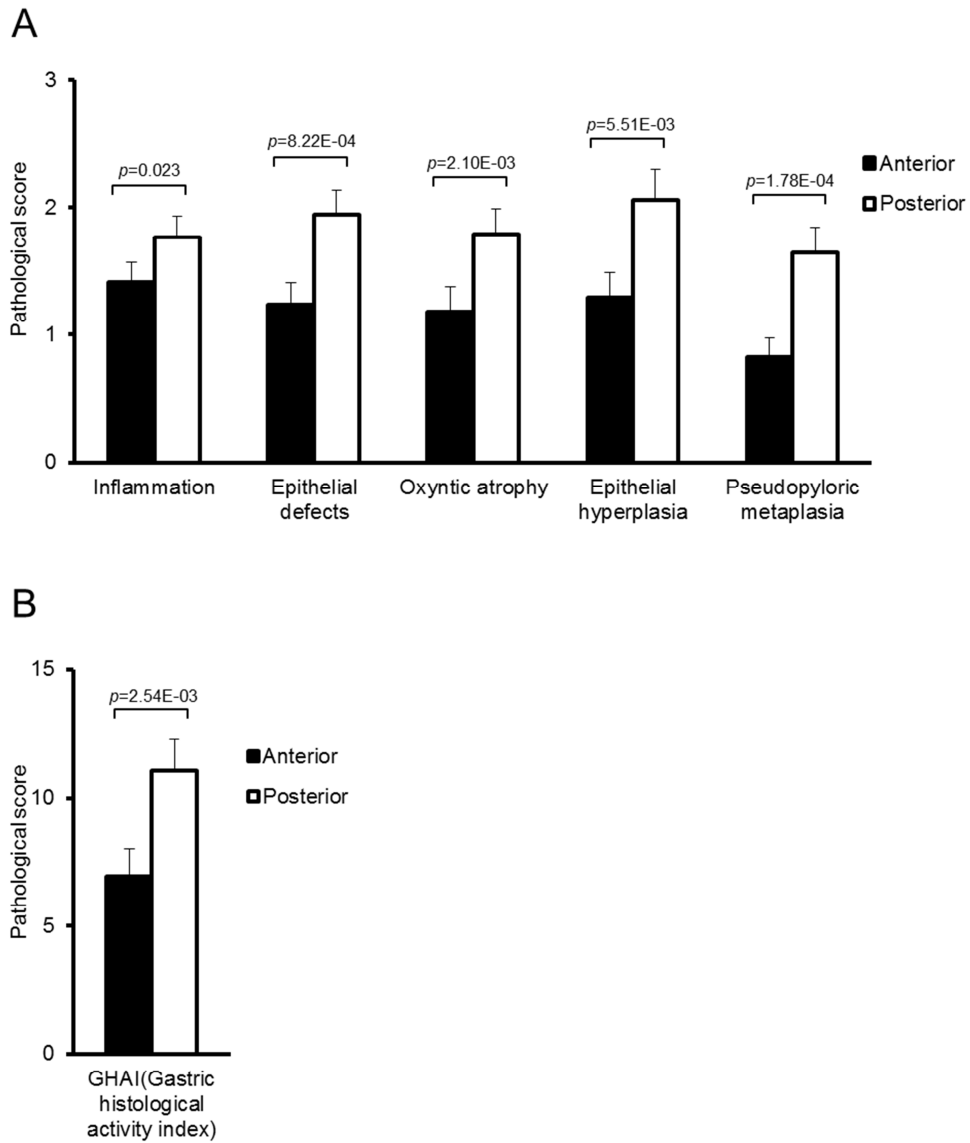


Figure S6: Pathological scores for the stomach after Botox injection in INS-GAS mice. Pathological scores for inflammation, epithelial defects, oxyntic atrophy, epithelial hyperplasia, pseudopyloric metaplasia (A), and GHAI (gastric histological activity index) (B) in Botox-injected (in anterior side of the stomach) INS-GAS mice at 12 months of age (monthly Botox injection starting at 6 months of age). Means \pm SEM ($N = 16$). Paired t test between anterior vs. posterior sides.

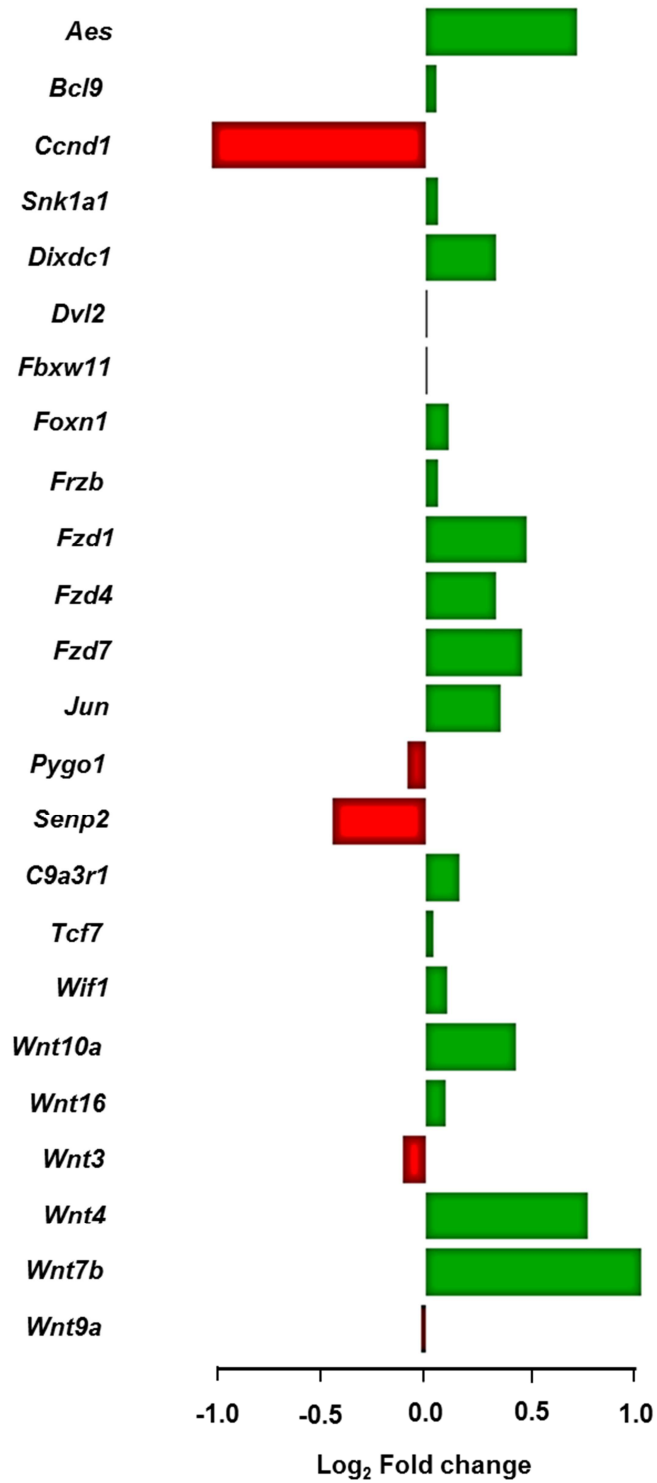


Figure S7: Wnt signaling in INS-GAS mice compared with wild-type mice. Fold changes of

Wnt-related genes: upregulated (indicated by red) and downregulated (green).

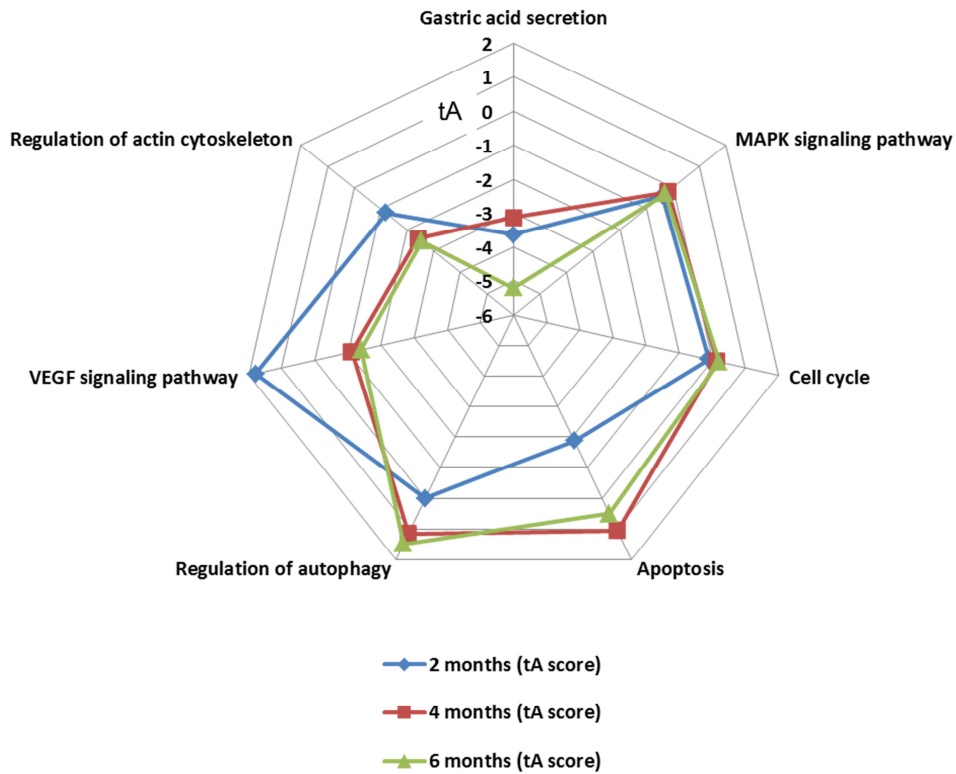


Figure S8: Altered signaling pathways after vagotomy in INS-GAS mice. Altered signaling pathways involved gastric acid, MAPK signaling, and tissue homeostasis at 2 (blue), 4 (green), and 6 (red) months in the anterior oxyntic mucosa of the stomach after anterior unilateral vagotomy compared with posterior side. tA score: -4 to 6. tA score>0: activation; tA score<0: inhibition.

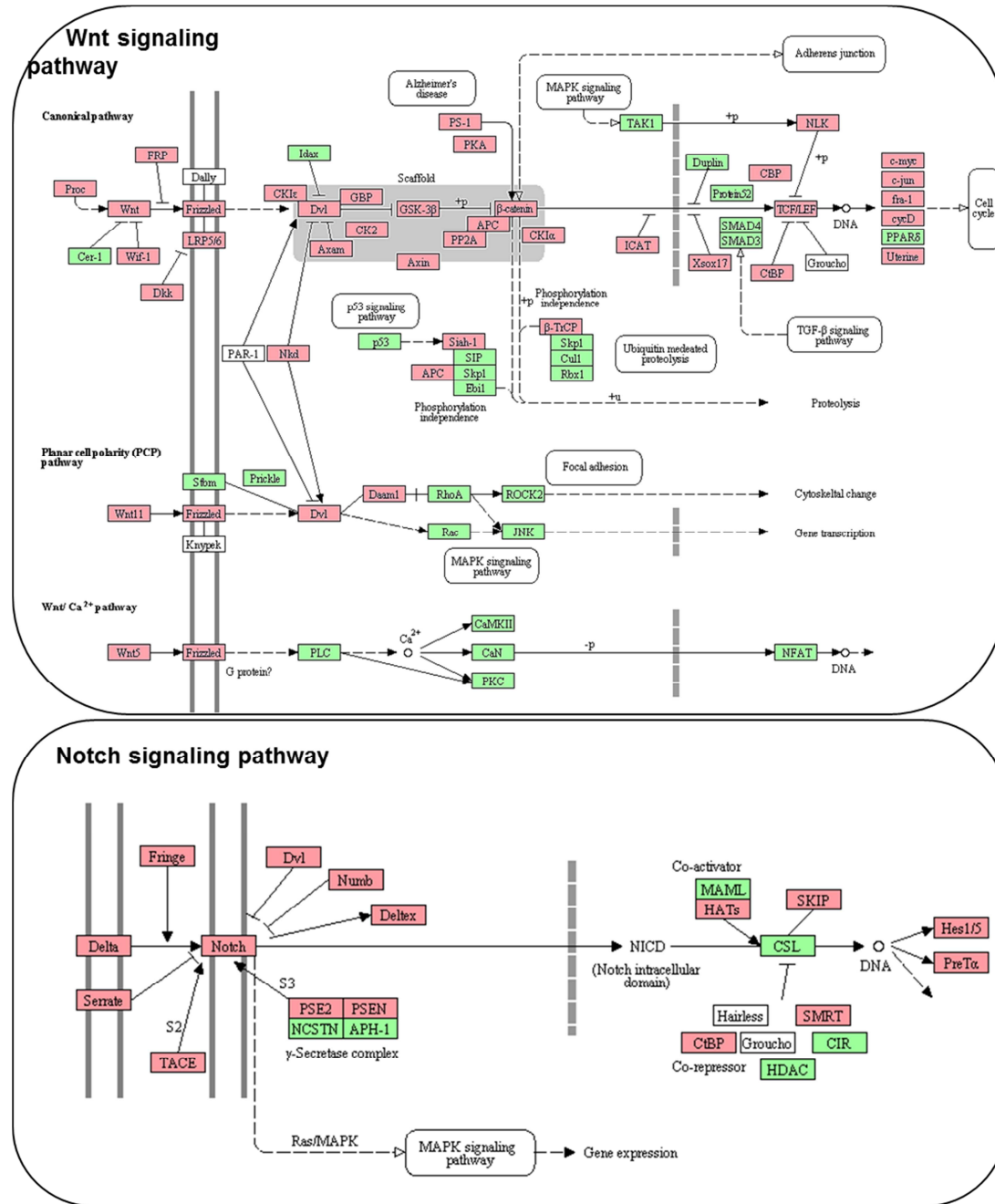


Figure S9: Wnt and Notch signaling pathways in the stomach after vagotomy in INS-GAS mice. Wnt and Notch signaling KEGG pathways in the anterior oxyntic mucosa after anterior unilateral vagotomy compared with the posterior side at 6 months postoperatively. Down-regulated genes ($p < 0.05$) are indicated by pink; unchanged genes are green.

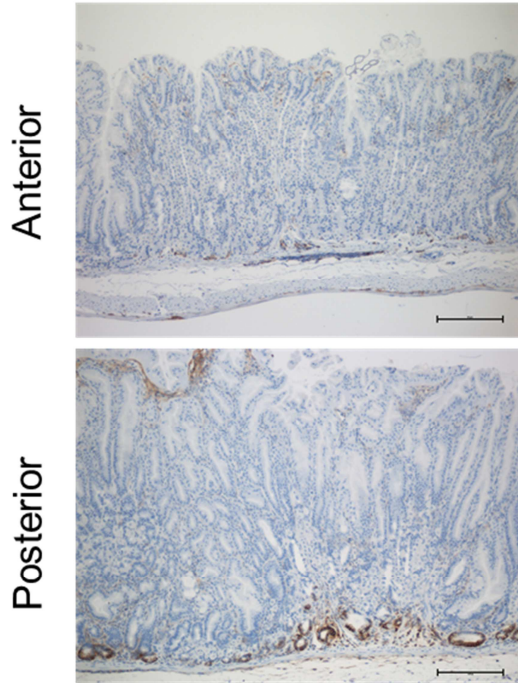


Figure S10: Immunostaining of CD44 after vagotomy in INS-GAS mice. Representative microphotographs of CD44+ cells in the oxyntic mucosa of the anterior and the posterior regions of the same stomach in a mouse subjected to unilateral anterior vagotomy (UVT).

Scale bars = 25 μ m.

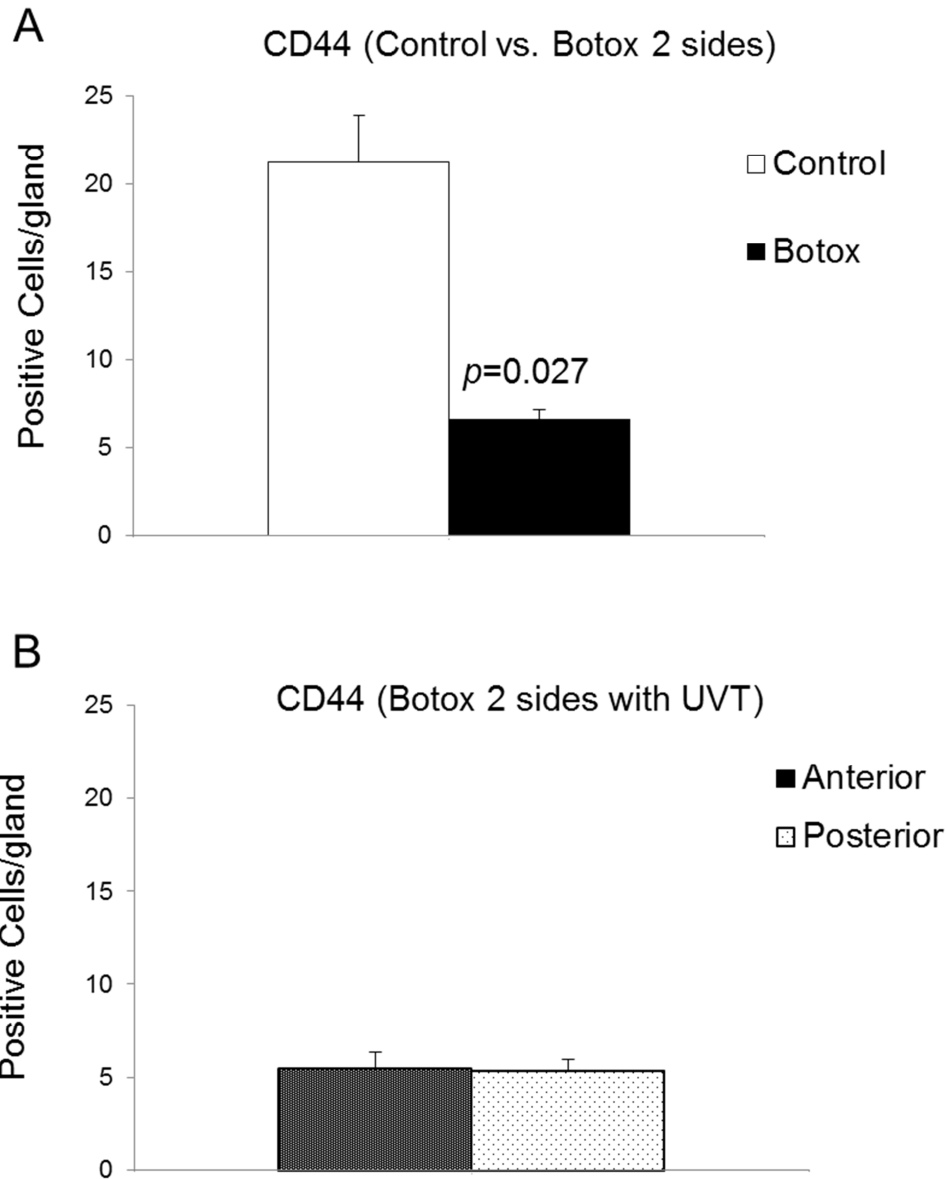


Figure S11: Numbers of CD44-immunoreactive cells after Botox treatment ± vagotomy in INS-GAS mice. CD44-immunoreactive cells in mice subjected to saline (control) or Botox injection into anterior and posterior sides of the stomach (A) and Botox injection into anterior and posterior sides plus anterior UVT (B). Means ± SEM. Student's *t* test was used to compare control ($N = 6$) and Botox ($N = 7$).

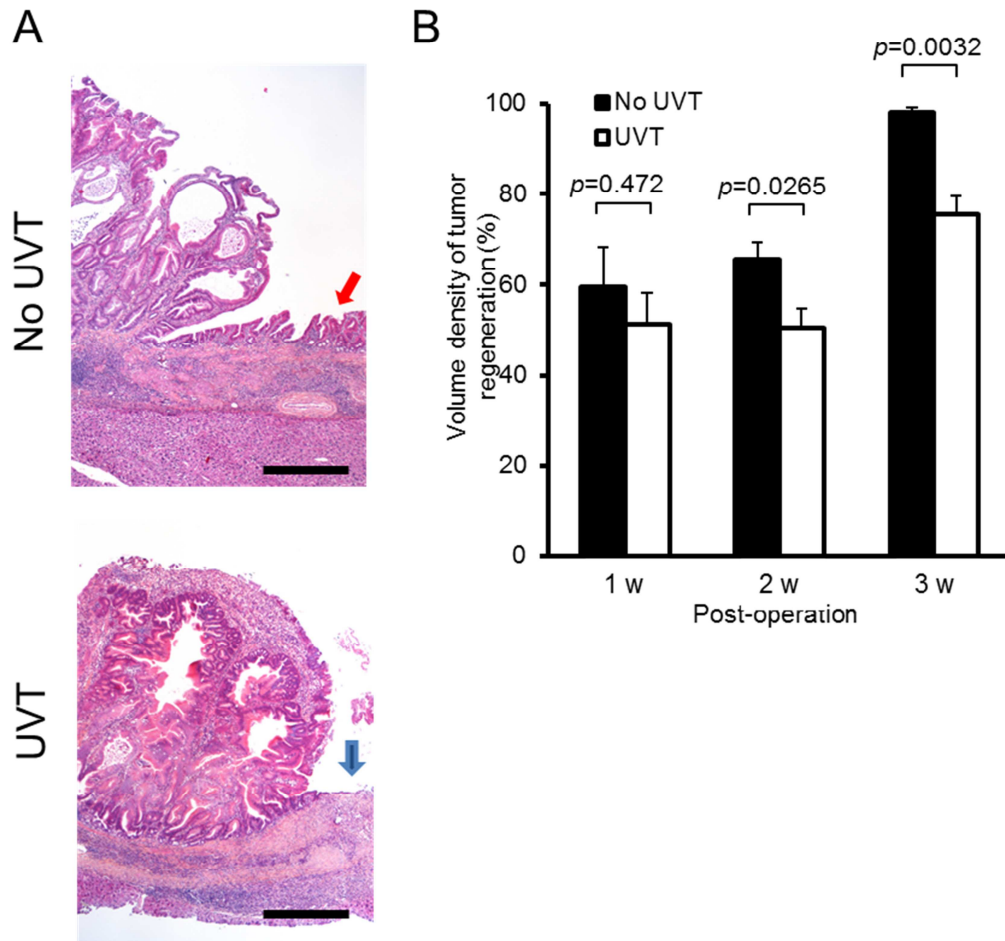


Figure S12: Tumor regeneration in the stomach after vagotomy in INS-GAS mice. (A) Microphotographs showing histopathological appearances of tumor regeneration at 3 weeks after acetic acid-induced necrotic ulcer. Note regeneration (indicated by red arrow) without unilateral vagotomy (No UVT) and no regeneration (blue arrow) after UVT. Scale bars: 50 μm . (B) Volume density of tumor regeneration 1, 2, and 3 weeks after application of acetic acid in mice with or without UVT. Means \pm SEM. Student's *t* test was used to compare no UVT and UVT ($N = 6$, except $N = 8$ or 5 , respectively, at 3 weeks).

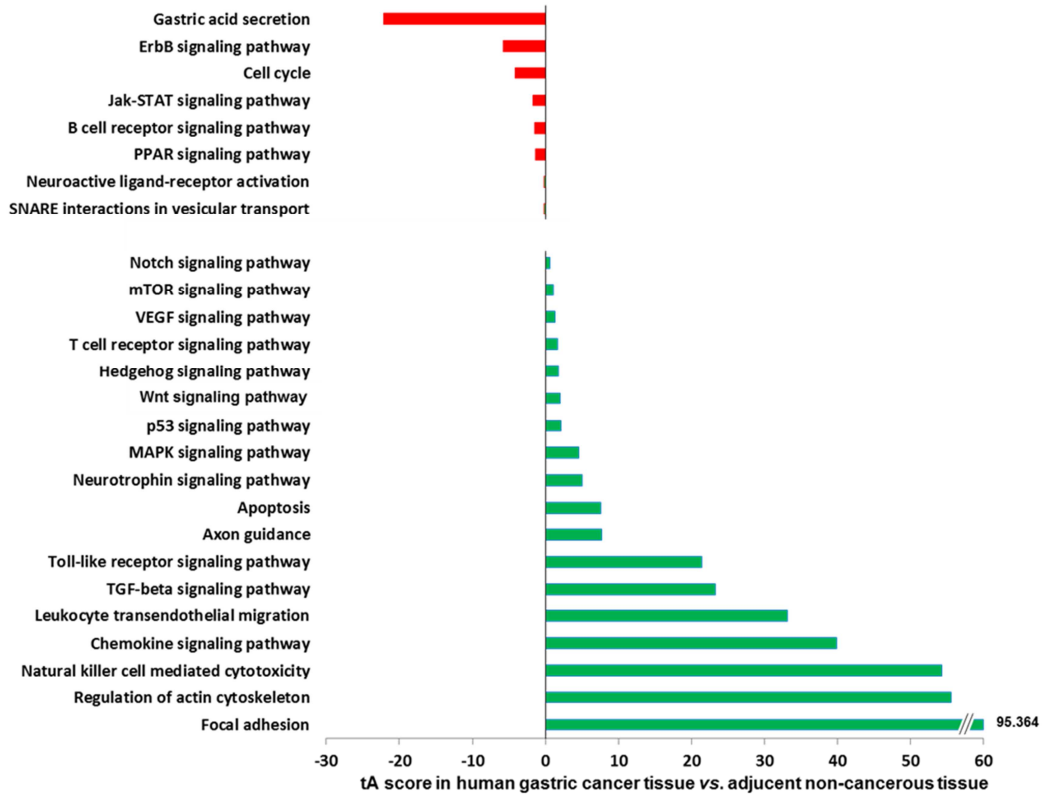
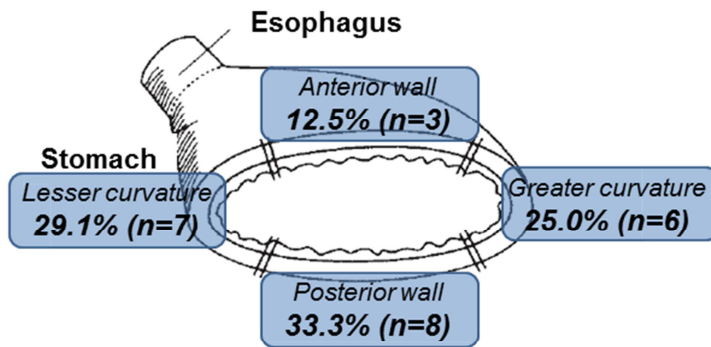


Figure S14: Altered signaling pathways in human gastric cancer tissue compared with adjacent noncancerous tissue. tA score>0: activation (indicated by green); tA score<0: inhibition (red)

A Non-vagotomized patients (n=24)



B Vagotomized patients (n=13)

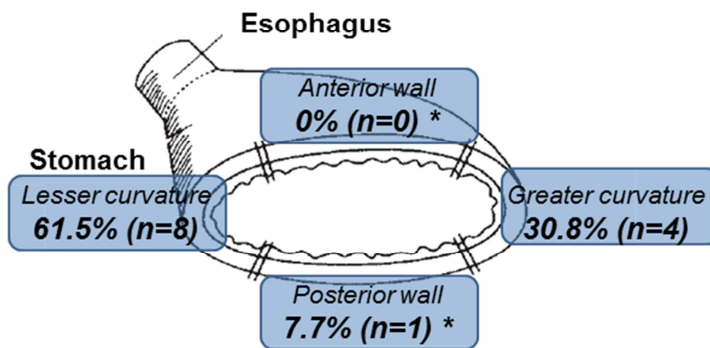


Fig. S15. Gastric stump cancer after distal gastrectomy with or without vagotomy. (A) Tumors in both anterior and posterior walls in 24 patients without vagotomy. (B) No tumors in anterior and one tumor in a posterior wall among 13 patients who underwent vagotomy. $p = 0.01898$ or $p = 0.02718$ for anterior or posterior wall of vagotomized patients compared with non-vagotomized patients (Fisher test).

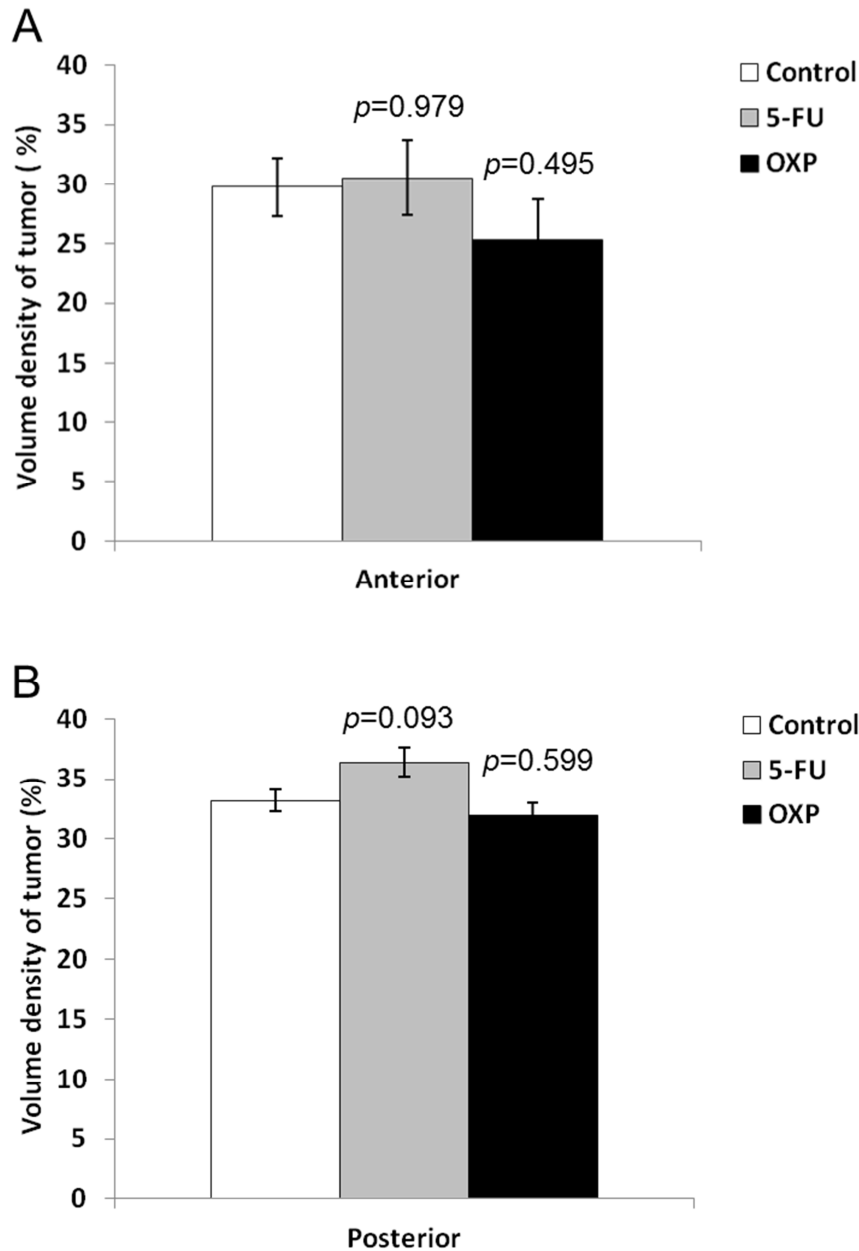


Fig. S16. Effect of 5-FU and oxaliplatin on INS-GAS mice. Tumor size in the anterior (A) or posterior (B) sides of stomachs in mice treated with saline (Control, $N = 10$), 5-FU ($N = 10$), or oxaliplatin (OXP, $N = 13$). Means \pm SEM. P values were calculated by Dunnett's test.

Table S1. Animal experimental groups.

	Mouse (N)	Group (N)	Age* at operation (months)	Age* at examination (months)
1	INS-GAS (107)	Sham (27)	6	12
		PP (25)	6	12
		UVT (30)	6	12
		VTPP (25)	6	12
2	MNU (FVB)(20)	MNU+ PP(11)		13
		MNU+VTPP (9)	3.5	13
3	<i>H.p.</i> -infection (24)	Sham (12)	12	18
		UVT (12)	12	18
4	INS-GAS (16)	UB (16)	6	12
5	INS-GAS (64)	No surgery (21)		18
		UVT (17)	8	18
		UVT (14)	10	18
		UVT (12)	12	18
6	INS-GAS (26)	Vehicle (6)	12	14
		UB (6)	12	14
		BB (7)	12	14
		BB+UVT (7)	12	14
7	INS-GAS (133)	No treatment (12)	12-14	14-16
		Saline (10)	12-14	14-16
		5-FU (10)	12-14	14-16
		OXF (13)	12-14	14-16
		UB+Saline (10)	12-14	14-16
		UB+5-FU (10)	12-14	14-16
		UB+OXF (13)	12-14	14-16
		Sham+5-FU+OXF (15)	12-14	14-16
		UB+5-FU+OXF (24)	12-14	14-16

	UVT+5-FU+OXP (16)	12-14	14-16
8	INS-GAS (16)		
	UVT (5)	6	8
	UVT (5)	6	10
	UVT (6)	6	12
9	INS-GAS (64)		
	Saline (19)	12-14	14-16
	5-FU+OXP (12)	12-14	14-16
	Darifenacin (15)	12-14	14-16
	5-FU+OXP+darifenacin (8)	12-14	14-16
10	INS-GAS (12)	INS-GAS - No treatment (6)	6
	FVB (20)	INS-GAS - UVT (6)	6
		WT- No treatment (10)	6
		WT- UVT (10)	6
11	MNU (12)		
	PP (6)	6	10
	VTPP (6)	6	10
12	M3KO (7)	M3KO+MNU (7)	11
	C57BL/6 (13)	WT+MNU (13)	11
13	INS-GAS (37)		
	Regeneration** 1 week (6)	12-18	12-18+1week
	Regeneration 1 week after UVT (6)	12-18	12-18+1week
	Regeneration 2 weeks (6)	12-18	12-18+2weeks
	Regeneration 2 weeks after UVT (6)	12-18	12-18+2weeks
	Regeneration 3 weeks (8)	12-18	12-18+3weeks
	Regeneration 3 weeks after UVT (5)	12-18	12-18+3weeks
14	Lgr5-GFP (10)		
	MNU + PP (5)	4,75	6,25
	MNU+ VTPP (5)	4,75	6,25

PP: Pyloroplasty, UVT: Unilateral vagotomy, VTPP: Bilateral vagotomy+pyloroplasty

UB: Unilateral Botox injection, BB: Bilateral Botox injection, OXP: Oxaliplatin

*Preneoplasia at 6 months and neoplasia at 12 months of age in INS-GAS mouse. **Tumor regeneration was induced by topical application of acetic acid.

Table S2. Cohorts of gastric cancer patients.

	1st cohort	2nd cohort	3rd cohort
Country	Norway	Japan	Japan
Purpose	Gene expression profiling	Innervation and tumorigenesis	Stump cancer after vagotomy
Study period	2005-2010	2001-2008	1962-1998
Patient			
Number (male:female)	17 (14:3)	120 (78:42)	37 (31:6)
Age (y.o.)	49-86	31-92	69-90
Pathological stage	I-IV	II-IV	I-II
<i>H.pylori</i> status	10/17 positive	n.d.	n.d.

Table S3. List of qRT-PCR primers used in this study.

Gene	Forward (5'->3')	Reverse (5'->3')
<i>Lgr5</i>	TCCAACCTCAGCGTCTTC	TGGGAATGTGTGTCAAAG
<i>Cd44</i>	CACATATTGCTTCAATGCCTCAG	CCATCACGGTTGACAATAGTTATG
<i>Axin2</i>	ACTGACCGACGATTCCATGT	TGCATCTCTCTCTGGAGCTG
<i>Myc</i>	AGAGCTCCTCGAGCTGTTTG	TGAAGTTCACGTTGAGGGG
<i>Cyclin D1</i>	TCCTCTCCAAAATGCCAGAG	GGGTGGGTTGGAAATGAAC
<i>Sox9</i>	AGGAAGCTGGCAGACCAGTA	TCCACGAAGGGTCTCTTCTC
<i>Chrm1</i>	CAGAAGTGGTGATCAAGATGCCTAT	GAGCTTTTGGGAGGCTGCTT
<i>Chrm2</i>	TGGAGCACAACAAGATCCAGAAT	CCCCTGAACGCAGTTTTCA
<i>Chrm3</i>	CCAGTTGGTGTGTTCTTCCTT	AGGAAGAGCTGATGTTGGGA
<i>Chrm4</i>	GTGACTGCCATCGAGATCGTAC	CAAACCTTCGGGCCACATTG
<i>Chrm5</i>	GGCCCAGAGAGAACGGAAC	TTCCCGTTGTTGAGGTGCTT
<i>Gapdh</i>	TCATTGTCATACCAGGAAATGAG	AGAAACCTGCCAAGTATGATGAC